PROCEEDINGS, 43rd Workshop on Geothermal Reservoir Engineering
Stanford University, Stanford, California, February 12-14, 2018
SGP-TR-213

Potential Field Poisson Wavelet Multiscale Edge Analysis (Worms) for Geothermal; A Review

Franklin G. Horowitz

Dept. EAS, Cornell University, Ithaca, NY 14853, USA

frank@horow.net

Keywords: Gravity, Magnetics, Wavelets, Geophysics, Induced Inversion

ABSTRACT

Gravity and magnetic potential field methods have a long history in geothermal technologies and elsewhere. The traditional approach is to take the measurements, grid them, invert them – using some canned procedure – and then to interpret the results. Starting about 20 years ago in mineral exploration, a wavelet-based approach short-circuited the inversion and produced results directly interpretable as lateral contacts in the underlying rocks. This talk will present a brief overview of the technique's underpinnings, and then show case studies of interest in geothermal activities. One case study will demonstrate the technique directly detecting a blind structure with injection-correlated seismicity in the Avoca region of Upstate New York, USA. Another case study correlates worm detected structures with those identified by seismic reflection in a geothermal exploration project near Wiesbaden in Germany.

1. INTRODUCTION

Poisson wavelet multiscale edge analyses of potential fields – informally, "worms" for brevity – were described in the literature about twenty years ago (Hornby et al., 1999; independently derived by Moreau et al., 1997). Broadly speaking, the technique has formed the basis for two different classes of usage. The first class is subsequent theoretical development of auxiliary results – following the rather mathematical descriptions in the original papers. Here, I will concentrate on a second class – the use of worms as an aid for interpreting potential fields.

Interpreting potential fields has a long and detailed history (e.g. Blakely, 1996, and the references therein). What worms bring to the table is a visual display of multiple scales and classes of discontinuities in the underlying rocks. After relatively brief training, experience in the Australian mineral exploration community has demonstrated that geologists and other people interested in the 3D geological structures are adept at interpreting worms – often without the aid of detailed geophysical training. This is primarily because worms perform a "no tweaking of parameters" *induced* inversion of potential fields under a regularizing assumption that "rocks have edges". The result is the location of "apparent lateral property contrasts" in the underlying rocks. Geologically, these contrasts correspond to faults or other relatively steeply dipping contacts – with some important caveats to be described below.

2. OVERVIEW OF WORMS

2.1 Descriptive Version

Operationally, for gravity the worm technique from original Hornby et al. (1999) paper takes a Bouguer gravity grid, upward continues it to a suite of heights, then detects local maxima in the horizontal gradient of the results at each height, marking those locations as multiscale edges. Similarly, for magnetic surveys, a pseudogravity transform grid is used instead of a Bouguer grid. Hornby et al. (1999) show that – to within a factor – upward continuation *is* a wavelet scale change, effectively marrying potential field theory and wavelet theory together.

Later theoretical work (Boschetti et al., 2001; Hornby et al., 2002) identified a physical interpretation of the gravity Poisson wavelet transform itself. In essence, the gravity field wavelet is (proportional to) a Green's function for mass dipoles. Hence, via the inverse wavelet transform (equation B6 in Hornby et al., 1999), the observed field is proportional to the field generated by a distribution of sources composed entirely of horizontal mass dipoles. The depths of the dipoles are equal to the negative of the height of upward continuation. The multiscale edges then correspond to local peaks of the probability density of the horizontal dipole source distribution induced by the wavelet transform.

A geological interpretation as locations of "steeply dipping" fault or structural contacts follows naturally for multiscale edges from the very character of a horizontal dipole. Similarly, it follows naturally that the change with depth of the position of an edge marks the dip of the geological contact. A drawback of the technique is that the depth estimates are less reliable with increasing depth – due to the smoothing character of upward continuation.

Figure 1 shows a cartoon of the situation.

Like any potential field inversion technique, these induced source distributions are not unique, which leads us to some caveats.

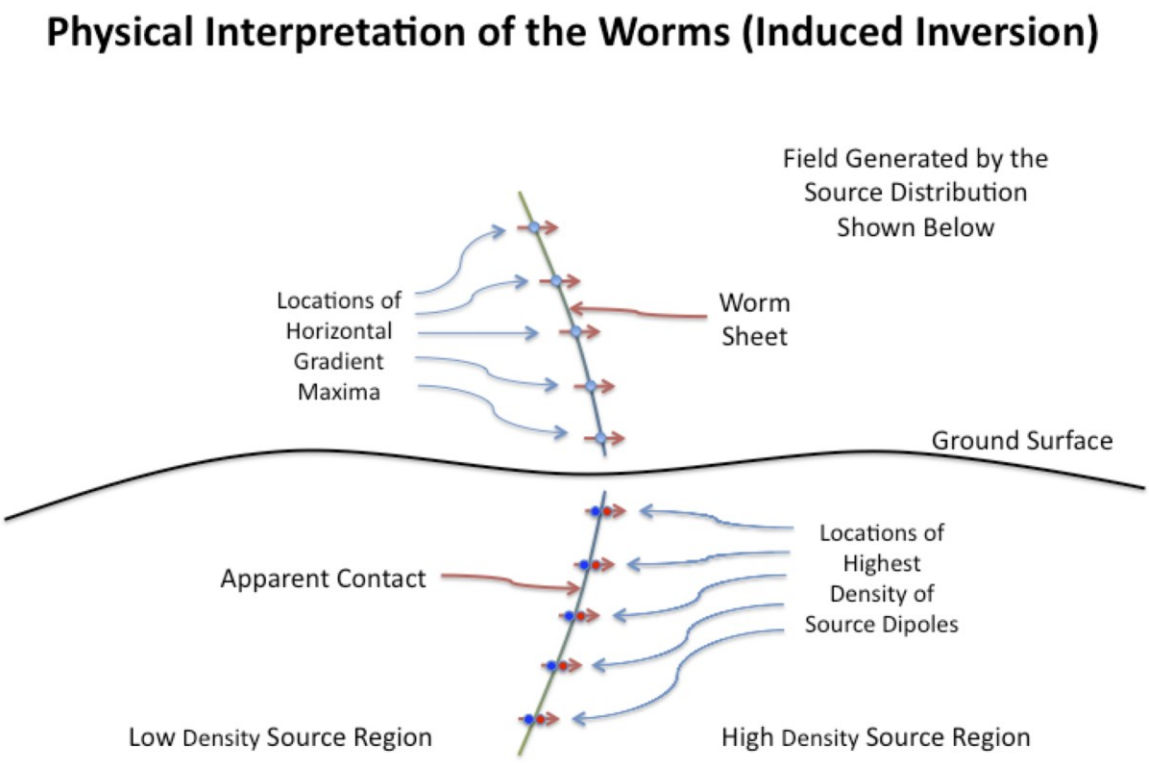

Figure 1: Cartoon vertical cross-section of worm edge detection. The (oriented) maximum horizontal gradient of a potential field at a suite of upward continued heights is found above ground. The same locations with heights swapped for depths are the locations of apparent faults or other lateral geological contacts underground. The above ground blue dots are worm points found as the local maxima of the horizontal field gradients. The worms themselves are the collection of worm points in to and out of the diagram – best seen in map view. If the z values being analyzed were continuous instead of a discrete set, the result would be a continuous worm sheet displayed above ground. Taking the exact same worm point locations and substituting –z for z so that the worms are underground yields the locations of the dipole sources described in the text.

2.2 Mathematical Version

For completeness, I include a condensed mathematical version of the same material as in the previous subsection. Consult Hornby et al. (1999) for the full details. The nonmathematical reader should feel free to skip this subsection on first reading.

The forward Poisson (first order) wavelet transform of a field (equation 2.22a of Hornby et al. 1999) is given by:

$$\vec{W}\left[f_0\right]\left(s,\vec{x}\right) = \left(z/z_0\right)\vec{\nabla}f_z\left(\vec{x}\right) \tag{1}$$

where f_0 is the scalar potential field of interest evaluated at a unit height z_0 above the sources, W is the wavelet transform, a 2D horizontal vector is denoted by an arrow over the symbol, x is the 2D position, s is the wavelet scale factor defined by $s=(z/z_0)$, $\vec{\nabla}$ is the 2D vector valued horizontal gradient, and f_z denotes the upward continuation to a height z of potential field f_0.

The modulus of the wavelet transform (equation 2.22b of Hornby et al., 1999) is defined by:

$$M\left[f_0\right]\left(s,\vec{x}\right) = \left\|\vec{W}\left[f_0\right]\left(s,\vec{x}\right)\right\| \tag{2}$$

where M denotes the modulus value and the norm is the 2D Euclidean distance.

The multiscale edges ("worms") are the collection of all local maxima of M at each height z. These edges are typically only evaluated at a discrete set of heights z for practical reasons.

The inverse wavelet transform is defined in equation B6 of Hornby et al. (1999) as:

$$f_0\left(\vec{x}\right) = 4\int_0^\infty \frac{ds}{s} \int_{\Re^2} \left(\vec{\psi}_s\left(\vec{u}-\vec{x}\right), \vec{W}\left[f_0\right]\left(s,\vec{u}\right)\right)_{\Re^2} d\vec{u} \tag{3}$$

where $\vec{\psi}_s$ is the actual (2D, vector valued) wavelet function at scale *s*, and (,) denotes an inner product. As discussed in section 2.4.3 of Hornby et al. (1999), $\vec{\psi}_s$ is composed of the Green's function (point source) for a potential field that is upward continued to height z followed by taking a horizontal gradient. Now, in the case of gravity the point source has a monopole mass source. Equivalently, for magnetic fields that have been pseudo-gravity transformed, the point source is a monopole of magnetization. The gradient of a monopole field results in a dipole field, so $\vec{\psi}_s$ has a physical interpretation as the field due to a dipole source observed at the upward continuation height *z*. (An aside for aficionados of wavelets: $\vec{\psi}$ turns out to be *both* the analyzing *and* the synthesizing wavelet in the sense of Kaiser, 1994.)

Based upon this dipole source realization – as pointed out by Boschetti et al. (2001) and Hornby et al. (2002) – apart from normalizations, constants etc., one can interpret equation (3) as the field at height z_0 arising from a superposition of horizontally oriented source dipoles. That is, the wavelet transform itself is proportional to a possible source distribution. The wavelet transform has **induced** a valid source inversion! In this inversion, the local maxima of *M* serve to locate the positions of highest probabilities of dipoles of certain orientations. A natural interpretation is that those are the locations of lateral source discontinuities.

But those local maxima in *M* are exactly the locations of multiscale edges! This implies that if one drapes them underground instead of above the surface, one finds the locations of lateral source discontinuities in the induced inversion.

Please note that unlike a typical geophysical inversion, there is no regularization anywhere in this process. One simply identifies the locations of apparent lateral edges without imposing smoothness, or choosing an artificial function to minimize in addition to data misfit, or any of the other usual trickery of inverse problems that can be so damaging to accurate results. Indeed, Hornby, Boschetti, and I used to joke that our regularizing principle was simply that "rocks have edges".

2.3 Caveats

The inversion is still rife with ambiguity – like any potential field inversion. This is simply one of an infinite family of sources that exactly generates the field f_0.

The dipole source distribution is clearly wrong insofar as being fundamentally an upward continuation it gets smoother with depth. Nothing I know about real geology says that rocks fundamentally get smoother with depth.

The inversion is fundamentally insensitive to horizontal discontinuities. Lateral gradients simply do not resolve horizontal contacts. The inversion has been loosely described as being sensitive to "steeply dipping" discontinuities, but that is misleading. Depending on gridding resolution and a number of other variable details, dips of 30º and sometimes shallower are readily discernable. (See Jessell 2001 for examples.)

The inversion implicitly assumes that sources are isolated from one another. But that is never the case in the real world. Stronger sources off to one side of an edge can "shadow" its signature such that only the truly strong sources are identified.

The edge locations are much more accurate near the surface than at depth. This is due both to the strong sources effect just mentioned and to the effects of scale. Indeed, when a source is upward continued to a height/scale where the source is no longer resolvable, it disappears with a characteristic "bowl" signature in the worms, leaving only larger scale features evident. That is a complete artifact – not a signature of basin-like structures everywhere.

It is tempting, but incorrect, to assume that worms identify all dipping geological contacts. If there is no material property contrast across a contact, there is no possible discontinuity signal for the wavelets to identify. This is relevant for (e.g.) strike-slip faults where property contrasts may only be scattered at discrete locations along strike, but do not occur elsewhere.

Not all worms persist in strength – defined as the value of *M* – with upward continuation. Indeed, *M(z)* along worm sheets contains information classifying the kind of discontinuity (points, lines, sheets, fractals) and was the original focus of Hornby et al. (1999). Fortunately, 2D discontinuities do tend to persist with upward continuation, so faults and other contacts are discernable.

Now that some caveats have been laid out, let us see some examples of what worms are good for.

3. CASE STUDIES

I'll present two case studies using the worms of potential relevance to geothermal work. One defines previously unknown (apparent) faults or other structures that were involved in induced seismicity from fluid injection on a structure in the Avoca region of Western New York State in the US. The second one is from an integrated geothermal exploration study in the Wiesbaden region of the Rhine Graben in Germany.

3.1 The Avoca Induced Seismicity Sequence

Horowitz et al. (2017) analyze an induced seismic sequence in Upstate New York that occurred during January and February of 2001. A commercial natural gas storage facility was being developed. The plan was to solution-mine a salt layer to create the required storage volume. The brine resulting from the solution mining needed to be disposed of, and the operators injected the brine into a deep sandstone. Figure 2 shows the general location, while Figure 3 shows the worm analysis. There is a strong correlation between the earthquakes and a structure detected by the worms. There is also a strong correlation between worms and the injection well location. A strong argument could be made that had the operators known of the existence of that structure they should not have injected there.

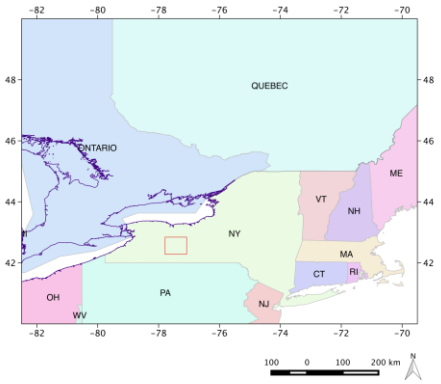

Figure 2: The red rectangle in the location map above shows the region mapped in Figure 3.

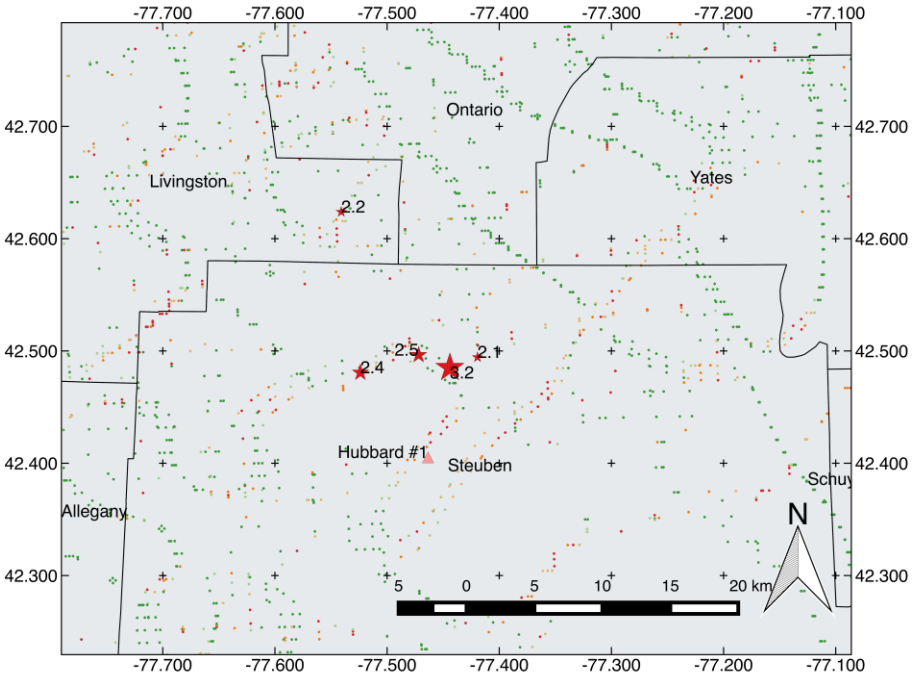

Figure 3: The dots represent locations at a suite-of-depths of worm points – faults or other lateral contacts. The colors represent an estimate of activation risk due to the local worm segment's orientation relative to an interpolation (due to Heidbach, et al. 2010) of the SHMax (largest horizontal stress) orientation from the World Stress Map. The light red triangle is the location of the Hubbard #1 injection well from the Avoca project. The stars are the locations of the seismic events with associated magnitudes. Note that the injection well is nearby a fault or other contact detected by the worm technique. Also note that seismic events are correlated with a different – possibly connected – structure detected by the worm technique. The Mb 3.2 event was teleseismically detected by the Lamont Cooperative Seismic Network. The other events' locations were from the Canadian Geological Survey's network. The locations of those weaker events are less precise due to their being south of the edge of the seismometer network.

3.1 The Weisbaden Exploration Project

Deckert et al. (2017) describe geothermal exploration in the Wiesbaden region of the Rhine Graben in Germany. The potential play is a fault bounded, possibly compartmentalized system of upwelling and outflow of hot water in the local Saar-Nahe basin. Geothermal hot springs in the area have been known since Roman times. However, the Deckert et al. work is the first to combine a gravity survey with 2D and 3D seismic reflection surveys to investigate the geological structures at depth.

For the purposes of this paper, the most relevant aspect of the Deckert et al. (2017) work is the coincidence between worm locations at depth and faults identified via seismic reflection. Figure 4 (below) reproduces Figure 7 from that work.

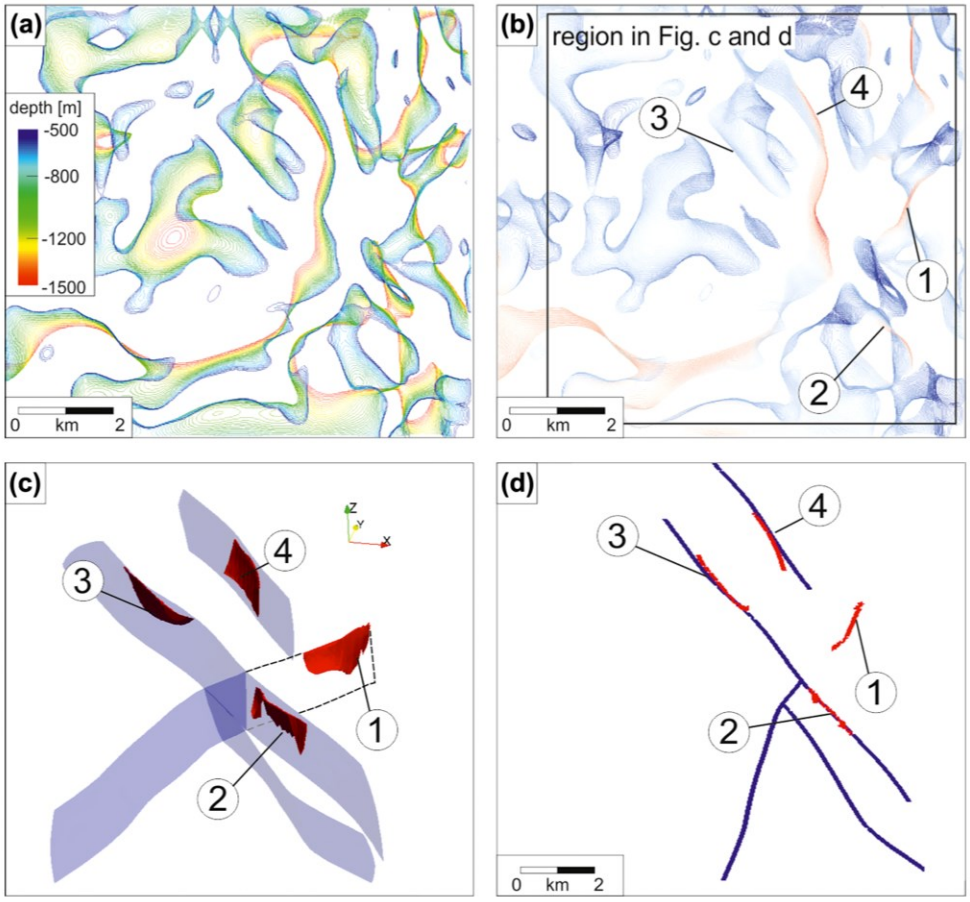

Figure 4: (Reproducing Figure 7 of Deckert et al., 2017). Multi-scale edges calculated from Bouguer gravity data. (a) Multi-scale edges for different depth levels (color coded) between 500 m and 1500 m depth. (b) Same view as in (a). Colors here depict amplitudes of multi-scale edges. Numbers are attributed to multi-scale edges, which follow prominent structures identified in 3D seismic reflection. (c) Prominent multi-scale edges combined to planes in red. Transparent blue planes show fault planes from the geological model based on 3D seismic data. Dashed black lines mark the interpreted continuation of a fault to an area that was not covered by 3D seismics but was covered by the gravity measurements. (d) Horizontal section in −750 m depth showing the consistency of seismic (blue) and multi-scale edges (red).

This example demonstrates that gravity worms and seismic reflection can co-locate structures of potential interest in an exploration context (Figure 4d). It also shows that the gravity survey might help interpret the extension of structures of interest beyond the boundaries of a seismic survey (the dashed lines in Figure 4c).

As mentioned in the Caveats section, the red oval of worms about 1/3 of the way East and halfway North in Figure 4a is an example of the "bowl" artifact produced when a feature is of too small a scale to be further resolved at depth.

3. DISCUSSION AND CONCLUSION

Both the Avoca and the Wiesbaden examples demonstrate that worms usefully locate blind "steeply" dipping structures that are corroborated via other techniques. In the Avoca example, the corroboration comes from the location of the induced earthquakes. In the Wiesbaden example, the corroboration comes from seismic reflection survey interpretations. It is worth mentioning that in both greenfields and brownfields exploration in the hard rock Australian mining context worms have proven their value repeatedly.

Software to compute the worms (Horowitz and Gaede, 2014) is BSD licensed and freely available from the bitbucket website at https://bitbucket.org/fghorow/bsdwormer.

REFERENCES

Boschetti, F., Hornby, P., & Horowitz, F. G. (2001). Wavelet Based Inversion of Gravity Data. *Exploration Geophysics*, *32,* (1), 48-55.

Blakely, R. J. (1996). Potential Theory in Gravity and Magnetic Applications. Cambridge: Cambridge University Press.

Deckert, H., Bauer, W., Abe, S., Horowitz, F. G., & Schneider, U. (2017). Geophysical greenfield exploration in the permo-carboniferous Saar-Nahe basin-the Wiesbaden geothermal project, Germany. Geophysical Prospecting, 44 (14), 17.

Heidbach, O., Tingay, M., Barth, A., Reinecker, J., Kurfeß, D., & Müller, B. (2010). Global crustal stress pattern based on the World Stress Map database release 2008. Tectonophysics, 482 (1-4), 3-15.

Hornby, P., Boschetti, F., & Horowitz, F. G. (1999). Analysis of potential field data in the wavelet domain. *Geophysical Journal International*, *137* (1), 175-196.

Hornby, P., Horowitz, F. G., & Boschetti, F. (2002). A physical interpretation of the Poisson wavelet transform of potential fields. In Proceedings, EGS XXVII General Assembly. European Geophysical Society, Munich: European Geophysical Society. http://www.cosis.net/abstracts/EGS02/05568/EGS02-A-05568.pdf

Horowitz, F. G., & Gaede, O. (2014). BSDWormer; an open source implementation of a Poisson wavelet multiscale analysis for potential fields. In 2014 Fall Meeting, T43C-4743. American Geophysical Union. http://abstractsearch.agu.org/meetings/2014/FM/T43C-4743.html

Horowitz, F. G., Ebinger, C., & Jordan, T. E. (2017). Identifying faults associated with the 2001 Avoca induced(?) seismicity sequence of western New York state using potential field wavelets. In 2017 Fall Meeting, (pp. S23C-0835+). American Geophysical Union. http://dx.doi.org/10.13140/RG.2.2.33567.05287

Jessell, M. (2001). An atlas of structural geophysics II. Journal of the Virtual Explorer, 05. http://virtualexplorer.com.au/journal/2001/05

Kaiser, G. (1994). A Friendly Guide to Wavelets. Boston: Birkhäuser.

Moreau, F., Gibert, D., Holschneider, M., & Saracco, G. (1997). Wavelet Analysis of Potential Fields. *Inverse Problems*, *13* , 165-178.